MODELLING OF DAMAGE IN FIBRE REINFORCED COMPOSITE LAMINATES UNDER MULTIAXIAL IN-PLANE LOADING

C. Soutis*, M. Kashtalyan, G.A.O. Davies
Department of Aeronautics, Imperial College of Science, Technology and Medicine, Prince Consort Road, London SW7 2BY, UK

Keywords: *fibre reinforced composite laminates, matrix cracking, delaminations, multiaxial loading, 2-D shear lag method, Equivalent Constraint Model*

Abstract

Resin-dominated damage modes, such as matrix cracking and delamination, are common failure mechanisms in composite laminates and are of primary concern in the current design with composites. Matrix cracking in the 90^o ply has long been recognised as the first damage mode observed in composite laminates under static and fatigue tensile as well as thermal loading. It results in reduction of the laminate stiffness properties and is detrimental to the laminate strength. It also triggers the development of other harmful damage modes, such as delaminations at the free edges of the laminate and/or local delaminations, growing from the tips of matrix cracks. Under biaxial or general in-plane loading, damage may affect more than one layer of the laminate, and different damage modes can interact with each other. Until now, multilayer damage of fibre-reinforced composite laminates has been very little modelled theoretically or simulated numerically (by means of the finite elements), mainly because the analysis of a representative element defined by the intersecting pairs of cracks is cumbersome. In the present paper, a new approach based on the Equivalent Constraint Model (ECM) of the damage lamina is applied to investigate multilayer matrix cracking and delaminations. It provides closed-form expressions for the reduced stiffness properties due to these damage modes. It will be shown that in carbon/epoxy laminates transverse and longitudinal cracking and delaminations cause significant reduction of the laminate shear modulus and Poisson's ratio, while the axial modulus is very little affected by the damage. Contribution of each damage mode into stiffness reduction will be established.

1 Introduction

Resin-dominated damage modes, such as matrix cracking and delamination, are common failure mechanisms in composite laminates and are of primary concern in the current design with composites. Matrix cracking in the 90^o ply has long been recognised as the first damage mode observed in composite laminates under static and fatigue tensile as well as thermal loading. It results in reduction of the laminate stiffness properties and is detrimental to the laminate strength. It also triggers the development of other harmful damage modes, such as delaminations at the free edges of the laminate and/or local delaminations, growing from the matrix crack tips.

When a laminate is subjected to biaxial or general in-plane loading, damage may affect more than one layer of the laminate, and different damage modes can interact with each other. In cross-ply $[0_m/90_n]_s$ laminates, transverse and longitudinal matrix cracks (splits) will appear in 90^o and 0^o plies respectively. They may be accompanied by

* Corresponding author

transverse and longitudinal delaminations growing along the respective matrix cracks at the $0^o/90^o$ interface. In cross-ply laminates reinforced by carbon fibres, these damage modes were observed also under uniaxial tension [1] as well as thermal loading [2].

Multilayer damage of fibre-reinforced composite laminates has been very little modelled theoretically or simulated numerically (by means of the finite elements), mainly because the analysis of a representative element defined by the intersecting pairs of cracks is very cumbersome. For cross-ply laminates, Hashin [3], Tsai and Daniel [4], [5], Henaff-Gardin, Lafarie-Frenot and Gamby [6] developed analytical models in order to predict stiffness reduction due to transverse and longitudinal cracking. None of these models takes into consideration delaminations growing at the $0^o/90^o$ interface along transverse and longitudinal cracks.

In the present paper, a model is developed for the analysis of cross-ply laminates, damaged by transverse and longitudinal matrix cracks and transverse and longitudinal delaminations growing along them. The model is based on the Equivalent Constraint Model (ECM) of the damaged ply [7] and employs an improved 2-D shear lag method [8] to determine the stress field in the damaged ply.

2 Damage Characterisation

A schematic of the damaged cross-ply $[0_m/90_n]_s$ laminate is shown in Fig. 1. Transverse and longitudinal cracks are assumed to be spaced uniformly and to span the full thickness and width of the 90^o and 0^o plies respectively, while transverse and longitudinal delaminations are assumed to be strip-shaped. Spacings between splits and transverse cracks are denoted respectively $2s_1$ and $2s_2$, and the strip widths of longitudinal and transverse delaminations are denoted $2\ell_1$ and $2\ell_2$, respectively. The laminate is subjected to biaxial tension ($\bar{\sigma}_{11}$ and $\bar{\sigma}_{22}$) and shear loading ($\bar{\sigma}_{12}$).

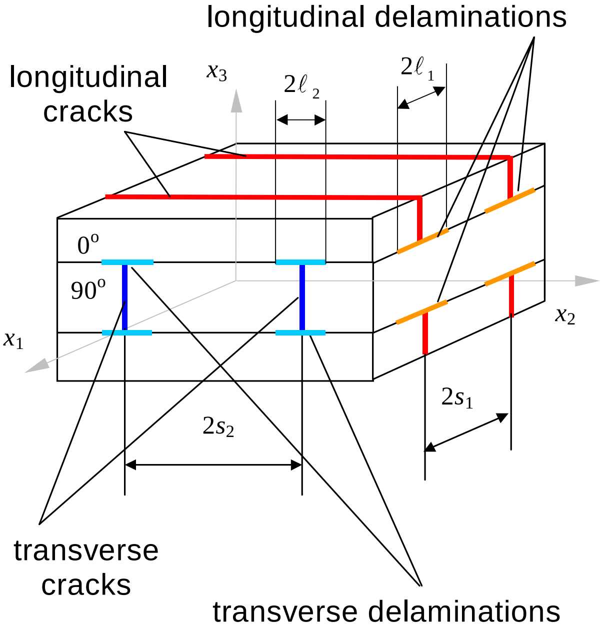

Figure 1. Cross-ply laminate damaged by transverse cracking, splitting and delaminations growing from the tips of transverse cracks and splits

3 Equivalent Constraint Model

Application of the Equivalent Constraint Model (ECM) of the damaged lamina to the problem means that the following two ECM laminates will be analysed instead of the damaged laminate configuration shown in Fig. 1. In the ECM1 laminate, the 0^o layer (1st layer) contains damage explicitly, while 90^o layer (2nd layer), damaged by transverse cracking and transverse delaminations, is replaced with the homogeneous one with reduced stiffness properties. Likewise, in the ECM2 laminate, the 90^o layer (2nd layer) is damaged explicitly, while the 0^o layer (1st layer), damaged by longitudinal matrix cracks and longitudinal delaminations, is replaced with the homogeneous one with reduced stiffness properties. ECM1 and ECM2 laminates are analysed simultaneously as a coupled problem. Their representative segments are shown in Fig. 2. These segments can be segregated into the locally delaminated ($0 < |x_\mu| < \ell_\mu$) and perfectly bonded ($\ell_\mu < |x_\mu| < s_\mu$) regions.

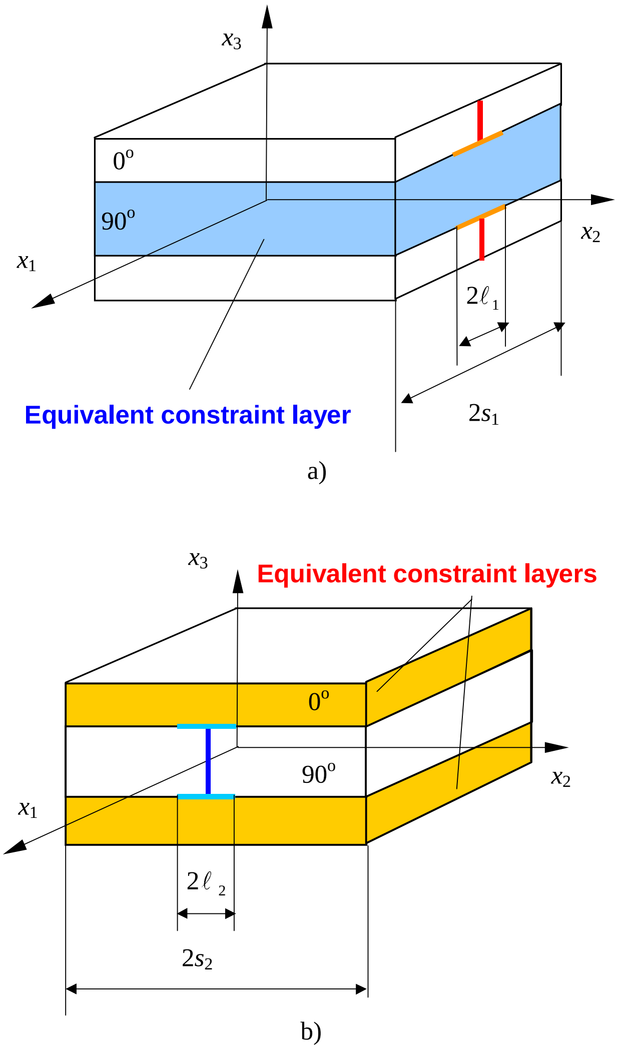

Figure 2: Representative segments of:
a) ECM1 laminate; b) ECM2 laminate

4 Stress analysis

The purpose of the analysis of an ECMμ laminate is to determine the reduced stiffness properties of the explicitly damaged μ^{th} ply. Let $\tilde{\sigma}_{ij}^{(\mu,k)}$, $\tilde{\varepsilon}_{ij}^{(\mu,k)}$ and $\tilde{u}_i^{(\mu,k)}$ denote respectively the in-plane microstresses, in-plane microstrains and the in-plane displacements in the k^{th} layer of the ECMμ laminate $(k,\mu=1,2)$, averaged across the thickness of the ply and width of the laminate.

Since crack and delamination surfaces are stress-free, stresses in the locally delaminated region of the explicitly damaged μ^{th} ply vanish. In the perfectly bonded region, they can be determined from the equilibrium equations

$$\frac{d}{dx_\mu}\tilde{\sigma}_{j\mu}^{(\mu,\mu)}+(-1)^\mu\frac{\tau_j^{(\mu)}}{h_\mu}=0,\quad j,\mu=1,2 \qquad (1)$$

where $\tau_j^{(\mu)}$ are the shear stresses at the $0^o/90^o$ interface of the ECMμ laminate in the j^{th} direction and h_μ is the layer thickness. It is assumed [8] that the out-of-plane shear stresses $\sigma_{j3}^{(\mu,k)}$, $j=1,2$ vary linearly across the thickness of the 90^o layer as well as over one-single-ply thickness t in the 0^o layer (so called shear layer)

$$\begin{aligned}\sigma_{j3}^{(\mu,2)}&=\frac{\tau_j^{(\mu)}}{h_2}x_3 \quad 0<|x_3|\le h_2,\quad j=1,2\\ \sigma_{j3}^{(\mu,1)}&=\frac{\tau_j^{(\mu)}}{t}(h_2+t-x_3)\quad h_2\le|x_3|\le h_2+t\end{aligned} \qquad (2)$$

By integrating the constitutive equations for the out-of-plane shear stresses $\sigma_{j3}^{(\mu,k)}$, $j=1,2$ (see Appendix of [9]), the interface shear stresses $\tau_j^{(\mu)}$ can be expressed as

$$\tau_j^{(\mu)}=K_j(\tilde{u}_j^{(\mu,1)}-\tilde{u}_j^{(\mu,2)}) \qquad (3)$$

$$K_j=\frac{3\hat{G}_{j3}^{(1)}\hat{G}_{j3}^{(2)}}{h_2\hat{G}_{j3}^{(1)}+(1+(1-\eta)/2)\eta h_1\hat{G}_{j3}^{(2)}} \qquad (4)$$

$$\eta=t/h_1$$

where $\hat{G}_{j3}^{(k)}, k=1,2$ are the out-of-plane shear moduli of the k^{th} layer, and K_j are the shear lag parameters. Substitution of shear lag equations (Eqs 3, 4) into equilibrium equations (Eqs 1) and subsequent differentiation with respect to x_μ yield

$$\begin{aligned}&\frac{d^2}{dx_\mu^2}\tilde{\sigma}_{\mu\mu}^{(\mu,\mu)}+(-1)^\mu\frac{K_j}{h_\mu}(\tilde{\varepsilon}_{\mu\mu}^{(\mu,1)}-\tilde{\varepsilon}_{\mu\mu}^{(\mu,2)})=0\\ &\frac{d^2}{dx_\mu^2}\tilde{\sigma}_{12}^{(\mu,\mu)}+(-1)^\mu\frac{K_j}{h_\mu}(\tilde{\gamma}_{12}^{(\mu,1)}-\tilde{\gamma}_{12}^{(\mu,2)})=0\end{aligned} \qquad (5)$$

Strain differences $(\tilde{\varepsilon}_{\mu\mu}^{(\mu,1)} - \tilde{\varepsilon}_{\mu\mu}^{(\mu,2)})$ and $(\tilde{\gamma}_{12}^{(\mu,1)} - \tilde{\gamma}_{12}^{(\mu,2)})$ can be expressed in terms of stresses $\tilde{\sigma}_{\mu\mu}^{(\mu,\mu)}$ and $\tilde{\sigma}_{12}^{(\mu,\mu)}$, using the equations of the global equilibrium of the laminate, constitutive equations for both layers, as well as the condition of generalised plane strain in the plane $Ox_\mu x_3$. Finally, Eqs. 5 are reduced to

$$\frac{d^2\tilde{\sigma}_{\mu\mu}^{(\mu,\mu)}}{dx_\mu^2} - L_1^{(\mu)}\tilde{\sigma}_{\mu\mu}^{(\mu,\mu)} + \mathbf{\Omega}_{11}^{(\mu)}\bar{\sigma}_{11} + \mathbf{\Omega}_{22}^{(\mu)}\bar{\sigma}_{22} = 0$$

$$\frac{d^2\tilde{\sigma}_{12}^{(\mu,\mu)}}{dx_\mu^2} - L_2^{(\mu)}\tilde{\sigma}_{12}^{(\mu,\mu)} + \mathbf{\Omega}_{12}^{(\mu)}\bar{\sigma}_{12} = 0 \qquad (6)$$

Here, $\bar{\sigma}_{ij}$ are the applied total stresses, $L_1^{(\mu)}, L_1^{(\mu)}, \mathbf{\Omega}_{11}^{(\mu)}, \mathbf{\Omega}_{22}^{(\mu)}, \mathbf{\Omega}_{12}^{(\mu)}$ are the constants depending on the compliances $\hat{S}_{ij}^{(\mu)}$ of the undamaged material of the explicitly damaged μ^{th} layer, modified (due to the implicitly contained damage) compliances $S_{ij}^{(\kappa)}, \kappa \neq \mu$ of the equivalent constraint layer(s), shear lag parameters K_j and the layer thickness ratio χ. In detail, they are presented in Appendix B of [9].

Given that at the boundary $|x_\mu| = \ell_\mu$ between locally delaminated and perfectly bonded regions of the ECMμ laminate the microstresses are zero, i.e. $\tilde{\sigma}_{\mu\mu}^{(\mu,\mu)} = \tilde{\sigma}_{12}^{(\mu,\mu)} = 0$, solutions of the differential Eqs. 6, i.e. microstresses in the perfectly bonded regions of the ECMμ laminate, are

$$\tilde{\sigma}_{\mu\mu}^{(\mu,\mu)} = \frac{1}{L_1^{(\mu)}} f_1(\chi_\mu, s_\mu, \ell_\mu)(\mathbf{\Omega}_{11}^{(\mu)}\bar{\sigma}_{11} + \mathbf{\Omega}_{22}^{(\mu)}\bar{\sigma}_{22})$$

$$\tilde{\sigma}_{12}^{(\mu,\mu)} = \frac{1}{L_2^{(\mu)}} f_2(\chi_\mu, s_\mu, \ell_\mu)\mathbf{\Omega}_{12}^{(\mu)}\bar{\sigma}_{12} \qquad (7)$$

$$f_j(\chi_\mu, s_\mu, \ell_\mu) = \left(1 - \frac{\cosh[\sqrt{L_j^{(\mu)}}(x_\mu - s_\mu)]}{\cosh[\sqrt{L_j^{(\mu)}}(s_\mu - \ell_\mu]}\right)$$

5 Material degradation estimation

The reduced stiffness properties of the damaged μ^{th} layer can be determined by applying the laminate plate theory to the ECMμ laminate after replacing the explicitly damaged layer with an equivalent homogeneous one. The modified in-plane stiffness matrix $[Q^{(\mu)}]$ of the homogeneous layer equivalent to the μ^{th} layer of the ECMμ laminate is related to the in-plane stiffness matrix $[\hat{Q}^{(\mu)}]$ of the undamaged layer as $[Q^{(\mu)}] = [\hat{Q}^{(\mu)}] - [\hat{R}^{(\mu)}][\Lambda^{(\mu)}]$, where

$$[\hat{R}^{(\mu)}] = \begin{bmatrix} \hat{R}_{11}^{(\mu)} & \hat{Q}_{12}^{(\mu)} & 0 \\ \hat{Q}_{12}^{(\mu)} & \hat{R}_{22}^{(\mu)} & 0 \\ 0 & 0 & \hat{Q}_{66}^{(\mu)} \end{bmatrix}$$
$$[\Lambda^{(\mu)}] = \begin{bmatrix} \Lambda_{22}^{(\mu)} & 0 & 0 \\ 0 & \Lambda_{22}^{(\mu)} & 0 \\ 0 & 0 & \Lambda_{66}^{(\mu)} \end{bmatrix} \qquad (8)$$

$$\hat{R}_{\mu\mu}^{(\mu)} = \hat{Q}_{\mu\mu}^{(\mu)}, \quad \hat{R}_{22}^{(1)} = (\hat{Q}_{12}^{(1)})^2(\hat{Q}_{11}^{(1)})^{-1}$$
$$\hat{R}_{11}^{(2)} = (\hat{Q}_{12}^{(2)})^2(\hat{Q}_{22}^{(2)})^{-1}$$

Here $\Lambda_{22}^{(\mu)}$, $\Lambda_{66}^{(\mu)}$ are the In-situ Damage Effective Functions (IDEFs) for the μ^{th} layer of the ECMμ laminate, for which the following expressions are derived

$$\Lambda_{qq}^{(\mu)} = 1 - \frac{1 - \mathbf{\Phi}_q(D_\mu^{mc}, D_\mu^{ld})}{\dfrac{1 + \beta_q^{(\mu)}D_\mu^{ld}}{1 - D_\mu^{ld}} + \gamma_q^{(\mu)}\mathbf{\Phi}_q(D_\mu^{mc}, D_\mu^{ld})} \qquad (9)$$

$$q = 2,6 \qquad \mathbf{\Phi}_q(D_\mu^{mc}, D_\mu^{ld}) =$$
$$= \frac{D_\mu^{mc}}{\beta_q^{(\mu)}(1 - D_\mu^{ld})} \tanh\left[\frac{\beta_q^{(\mu)}(1 - D_\mu^{ld})}{D_\mu^{mc}}\right] \qquad (10)$$

Here $D_\mu^{mc} = h_\mu / s_\mu$ and $D_\mu^{ld} = \ell_\mu / s_\mu$ are damage parameters, known respectively as crack density and relative delamination area.

Constants $\beta_q^{(\mu)}, \gamma_q^{(\mu)}$ depend solely on the layer compliances $\hat{S}_{ij}^{(\mu)}$, $S_{ij}^{(\kappa)}, \kappa \neq \mu$, shear lag parameters K_j and the layer thickness ratio χ. In detail they are given in [10]. IDEFs for the μ^{th} layer implicitly depend on the damage parameters $D_\kappa^{mc}, D_\kappa^{ld}$ associated with the equivalent constraint layer(s) through the modified compliances $S_{ij}^{(\kappa)}, \kappa \neq \mu$, which are determined from the analysis of the ECMκ laminate. IDEFs for both layers form a system of four simultaneous nonlinear algebraic equations, which is solved computationally by a direct iterative procedure.

6 Results and Discussion

Validation of the ECM/2-D shear lag approach in absence of delaminations is published elsewhere [11]. Here, the model is applied to examine stress fields and to predict degradation of stiffness properties in T300/934 laminates. Single ply properties of this carbon/epoxy material system are as follows: E_A=144.8GPa, E_T=11.38GPa, G_A=6.48GPa, G_T=3.45GPa, ν_A=0.3, ply thickness t=0.132mm.

Figure 3 shows stress distributions in $[0/90]_s$ and $[0/90_2]_s$ laminates under uniaxial and biaxial tension with different biaxiality ratios $\bar{\sigma}_{11}/\bar{\sigma}_{22} = 0; 1; 2$ ($\bar{\sigma}_{22} = 225\text{MPa}$). In-plane direct stresses $\tilde{\sigma}_{22}^{(2,2)}/Y_T$ in the 90$^{\text{o}}$ layer and $\tilde{\sigma}_{11}^{(1,1)}/Y_T$ in the 0$^{\text{o}}$ layers are normalised by the value of the transverse tensile strength Y_T and plotted as functions of the normalised distance from the crack x_μ/s_μ, $\mu = 1,2$. The transverse tensile strength for a T300/934 system is Y_T=45MPa. Crack/split density is 1 cm^{-1} in the $[0/90]_s$ laminate and 5 cm^{-1} in the $[0/90_2]_s$ laminate. It may be seen that, under biaxial loading, stresses in the cracked 0$^{\text{o}}$ and 90 layers are higher than under uniaxial loading. They increase with increasing biaxiality ratio and become larger than the transverse tensile strength of the material. This means that another crack will form without or with only a little increase in the applied load. At lower crack densities, stress curves exhibit a plateau, which means that, once the stresses reached the tensile transverse strength level, new crack may form over certain distance between two neighbouring cracks and not necessarily in the middle.

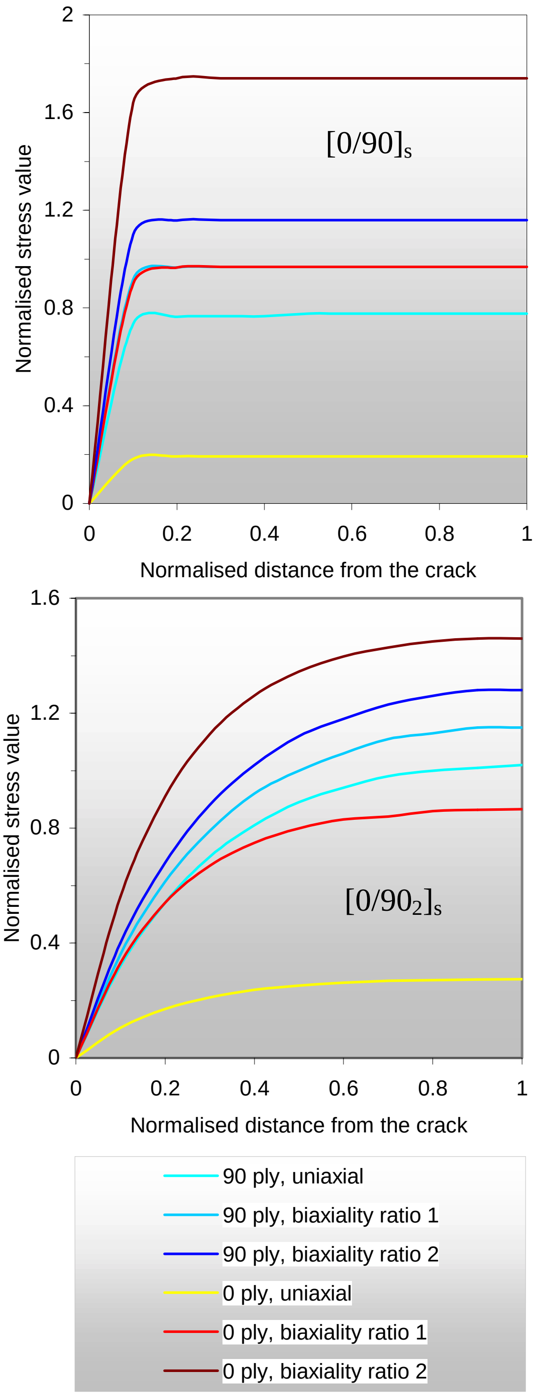

Figure 3 Normalised stresses in the 90$^{\text{o}}$ and 0$^{\text{o}}$ layers as a function of the normalised distance from the crack under uniaxial and biaxial tension for $[0/90]_s$ and $[0/90_2]_s$ T300/934 laminates

Figure 4 illustrates degradation of the laminate axial and shear moduli as well as Poisson's ratio due to transverse and longitudinal cracking (splitting) in $[0/90]_s$ and $[0/90_2]_s$ laminates. Properties reduction ratios are plotted as functions of transverse crack density. Two values of longitudinal crack density are considered; 0 splits/cm (i.e. no longitudinal cracking) and 10 splits/cm. Longitudinal cracking causes significant additional reduction of the laminate shear modulus and Poisson's ratio (Fig. 4b,c), but not of the axial modulus (Fig. 4a).

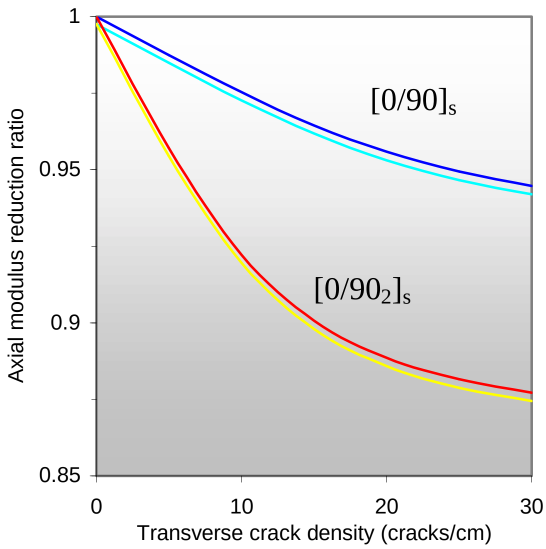

a)

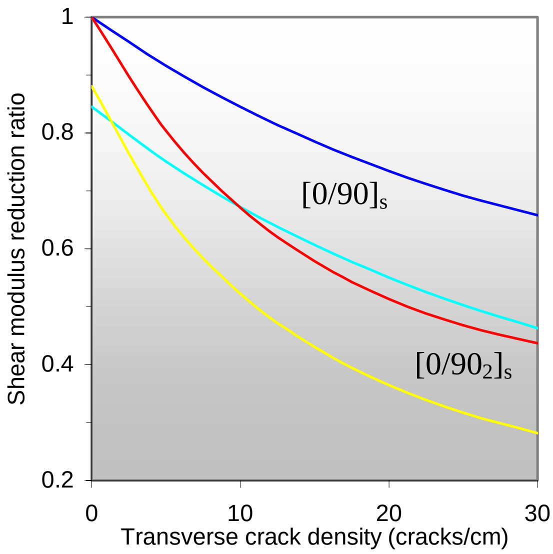

b)

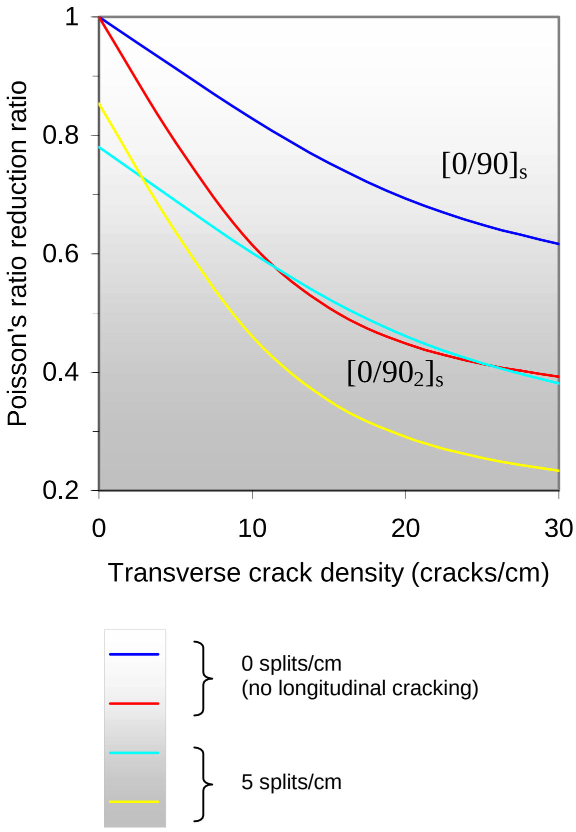

c)

Figure 4 Reduction ratios for the laminate axial and shear moduli and Poisson's ratio as function of transverse crack density for $[0/90]_s$ and $[0/90_2]_s$ T300/934 laminates. Longitudinal crack density 0 splits/cm (no longitudinal cracking) and 10 splits/cm

Figure 5 shows degradation of the laminate stiffness properties due to transverse and longitudinal delaminations that initiate and grow at $0^o/90^o$ interface respectively along transverse and longitudinal cracks in $[0_2/90_4]_s$ laminate. Reduction ratios for the axial and shear modulus and Poisson's ratio are plotted as functions of the relative delamination area. Transverse and longitudinal cracking is characterised by the same damage parameter value $D_1^{mc} = D_2^{mc} = 0.1$ This corresponds to transverse crack density of 0.95 cracks/cm and longitudinal crack density of 1.9 splits/cm. The area of transverse and longitudinal delaminations longitudinal cracking is taken to be equal, i.e. $D_1^{ld} = D_2^{ld}$.

As one may see, the laminate stiffness properties decrease linearly with increasing

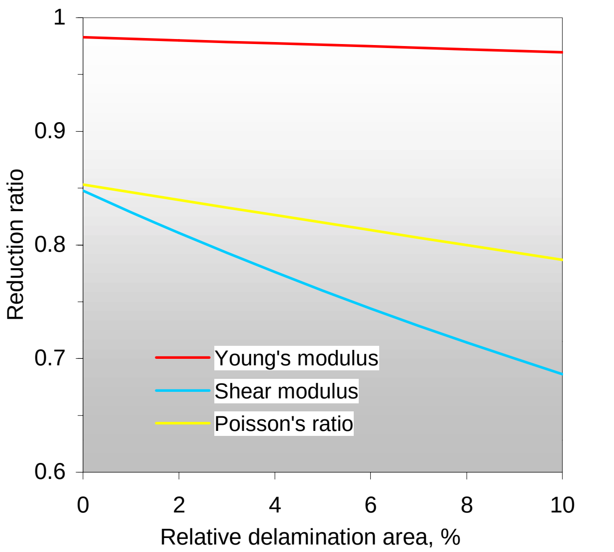

Figure 5 Reduction ratios for the laminate axial and shear moduli and Poisson's ratio as function of the relative delamination area for a $[0_2/90_4]_s$ T300/934 laminate. Damage parameters associated with transverse and longitudinal cracking $D_1^{mc}= D_2^{mc}$=0.1

delamination area. Shear modulus is reduced significantly, while axial modulus is almost unaffected. The total reduction of the axial modulus in this example is less than 5%, while the shear modulus is reduced by 34%, and the Poisson's ratio by 24%.

Figure 6 illustrates contribution of each damage mode (transverse cracking, longitudinal cracking, transverse delaminations, longitudinal delaminations) into the total reduction of the laminate stiffness properties when $D_1^{mc} = D_2^{mc} = 0.1$ and $D_1^{ld} = D_2^{ld} = 0.1$. The reduction of the axial modulus (Fig. 6a) occurs mainly due to transverse cracking and transverse delaminations, while the effect of longitudinal cracks and longitudinal delaminations is negligible. Transverse delaminations play the major role in the shear modulus reduction (Fig. 6b), though the contribution of transverse and longitudinal cracking is also significant. The Poisson's ratio (Fig. 6c) is reduced in equal parts by transverse and longitudinal cracking and transverse delaminations.

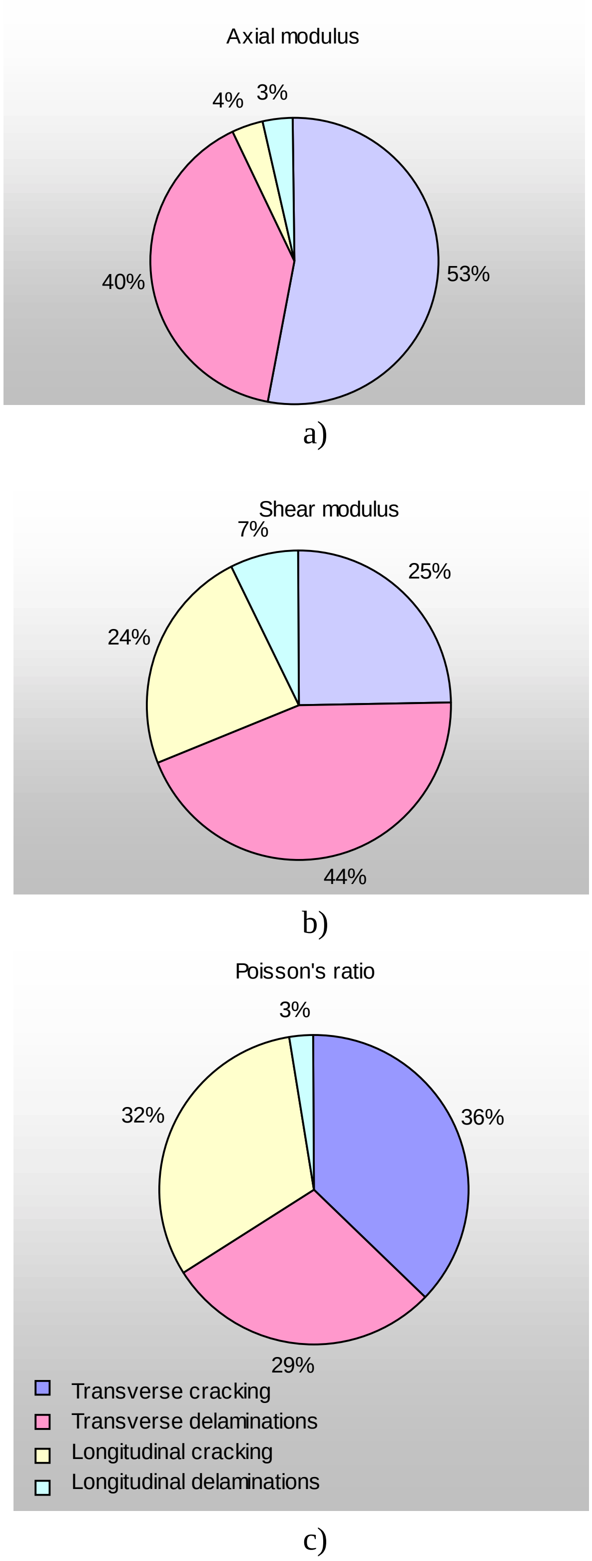

Figure 6 Damage mode contributions into the total reduction of the laminate stiffness properties of $[0_2/90_4]_s$ T300/934 laminates: a) axial modulus; b) shear modulus; c) Poisson's ratio. Damage parameters associated with transverse and longitudinal cracking are $D_1^{mc}= D_2^{mc}$=0.1, damage parameters associated with transverse and longitudinal delaminations are $D_1^{ld}=D_2^{ld}$=0.1

7 Concluding Remarks

To predict stiffness loss due to damage that occurs in fibre reinforced composite laminates under multiaxial loading, a new theoretical approach has been suggested, which takes into account interaction between damage modes in different layers. These include transverse and longitudinal cracking as well as transverse and longitudinal delaminations, growing at the interface along the cracks in a cross-ply laminate. The approach is based on the Equivalent Constraint Model (ECM) of the damaged ply, and uses an improved 2-D shear lag method to determine the stress field in the damaged layer.

The approach has been used to examine stresses and predict stiffness degradation in T300/934 cross-ply laminates. It is found that, under biaxial loading, stresses in the cracked plies are higher than under uniaxial loading, due to the stress transfer between the layers. Transverse and longitudinal cracking and delaminations cause significant reduction of the laminate shear modulus and Poisson’s ratio, while the axial modulus is very little affected by the damage. Contribution of each damage mode into stiffness reduction has been established.

Acknoledgements

Financial support of this research by Engineering and Physical Sciences Research Council (EPSRC/GR/L51348), Ministry of Defence and Hexcel Composites is gratefully acknowledged.

References

[1] Gyekenyesi A, Hemann J and Binienda W. Crack development in carbon polyamide cross-ply laminates under uniaxial tension. *SAMPE Journal*, Vol. 30, No. 1, pp. 17-28, 1994

[2] Henaff-Gardin C, Lafarie-Frenot MC and Gamby D. Doubly period matrix cracking in composite laminates Part 2: Thermal biaxial loading. *Composite Structures*, Vol. 36, No. 1, pp. 131-140, 1996

[3] Hashin, Z. Analysis of orthogonally cracked laminates under tension, *Transactions of the ASME. Journal of Applied. Mechanics*, Vol. 54, pp. 872-879, 1987

[4] Daniel IM and Tsai CL. Analytical/experimental study of cracking in composite laminates under biaxial loading, *Composites Engineering*, Vol. 1, pp. 355-362, 1991

[5] Tsai CL and Daniel I.M. Behavior of cracked cross-ply composite laminate under shear loading. *International Journal of. Solids and Structures*, Vol. 29, pp. 3251-3267, 1992

[6] Henaff-Gardin C, Lafarie-Frenot MC and Gamby D. Doubly period matrix cracking in composite laminates Part 1: General in-plane loading, *Composite Structures*, Vol. 36, pp. 113-130, 1996

[7] Fan J and Zhang J. In-situ damage evolution and micro/macro transition for laminated composites. *Composites Science and Technology*, Vol. 47, pp. 107-118, 1993

[8] Zhang J, Fan J and Soutis C. Analysis of multiple matrix cracking in $[\pm\theta_m/90_n]_s$ composite laminates Part 1: In-plane stiffness properties, *Composites*, Vol. 23, pp. 291-298, 1992

[9] Kashtalyan M and Soutis C. The effect of delaminations induced by transverse cracking and splitting on stiffness properties of composite laminates. *Composites Part A*, Vol. 31, No. 2, pp. 107-118, 2000

[10] Kashtalyan M and Soutis C. A study of matrix crack tip delaminations and their influence on composite laminate stiffness. *Advanced Composites Letters*, Vol. 8, No. 4, pp.149-156, 1999

[11] Kashtalyan M and Soutis C. Stiffness degradation in cross-ply laminates damaged by transverse cracking and splitting. *Composites Part A*, Vol. 31, No. 4, pp. 335-351, 2000